J-Researchers

Journal of Civil Engineering Researchers

Journal homepage: www.journals-researchers.com

Numerical Investigation of the Seismic and Axial Performance of Circular Steel Columns Filled with Double-Layer Concrete with Inner Bracing

Hadi Faghihmaleki,[a,*] Seyedeh Sara Farahpour[a]

[a] *Faculty of Civil Engineering, Ayandegan Institute of Higher Education, Tonekabon, Iran*

ABSTRACT

Concrete-filled double-shell circular steel columns consist of two concentric steel tubes with the space between them filled with concrete. These columns are a suitable option for high-rise construction due to their lower weight and also allow the passage of cables and utilities. In this research, modelling was carried out in Abaqus software and parametric analysis was performed based on variables such as the shape and dimensions of the stiffeners. The results show that concrete-filled double-shell columns perform better against axial and seismic loads than columns without concrete. The total and square stiffeners give the best performance, but it is not possible to increase their number due to space constraints. Trapezoidal stiffeners are also effective in improving axial and lateral performance, but result in a reduction in ductility. Circular stiffeners have the greatest reduction in ductility and their use is limited. In general, the choice of stiffener type has a significant effect on the performance of double shell columns.

ARTICLE INFO

Received: February 2, 2025
Accepted: April 1, 2025

Keywords:
Seismic Performance
Axial Performance
Double Shell Steel Column
Internal Stiffener
Finite Element Analysis

DOI: 10.61186/JCER.7.2.38
DOR: 20.1001.1.2538516.2025.7.2.4.2

1. Introduction

Concrete-filled double-shell steel columns (CFDST) have the advantages of concrete-filled steel columns (CFST) and are lighter, which is an advantage in high-rise construction due to their high performance with less weight [1]. In addition, the hollow section of these columns allows the passage of cables and utilities for power transmission towers and special structures [2]. The lighter weight and high efficiency of these columns has led to their use in applications such as offshore wind turbine support structures and tall power transmission towers. Concrete-filled double-shell steel columns (CFDST) are not yet common in our country due to their wide range of applications, which may call into question their practicality. Further research is needed to make these structures practical. One of the main disadvantages of CFST structures is that local buckling and delamination may occur under uniaxial compression due to the surface contact between concrete and steel. This problem may also

* Corresponding author. Tel.: +989112923228; e-mail: h.faghihmaleki@gmail.com.

be present in CFDST structures, but due to the presence of two inner and outer shells, it requires more detailed investigation in this area. One solution to reduce local delamination between concrete and steel is to use internal stiffeners. These stiffeners are installed in such a way that the two shells fit together easily, and then concrete is poured into the space between the two shells. The shape and dimensions of the stiffeners, as well as their spacing in the cross-section height, have a great influence on the seismic and axial performance of the columns [3,4].

Ding [5] showed that steel and steel sections can provide effective confinement for the core concrete. A study was also conducted on the effect of outer steel column confinement on the core concrete and the interaction between concrete and section steel, which showed that the models in Eurocode 4 may underestimate the load-bearing capacity of composite steel-concrete columns. Al-Ramaili et al. [6] showed that confinement by a steel column can significantly increase the load-bearing capacity of the column and inhibit diagonal shear cracking. Chitawadagi et al [7] in their research on 27 cold-rolled rectangular concrete filled steel columns found that increasing the wall thickness delayed local buckling failure. It increases the ultimate axial load capacity. Tawu et al. [8] performed a linear analysis of concrete filled square stainless-steel columns (CFSST) under axial compression and presented a formula for calculating the ultimate load capacity. Le Hewitt [9] used numerical methods to investigate the compressive behaviour of high-strength circular steel columns that had reached high strength by laboratory methods. Yuan et al. [10] presented an experimental investigation and numerical analysis of the performance of concrete-filled double-shell composite columns (CFDSCT) under axial loading.

This study investigates the effect of buried internal stiffeners in the cross-section of concrete-filled double-shell circular steel columns (CFDST) under compressive and lateral loading. In particular, this study addresses the reduction of local separation between concrete and steel in CFDST structures having two inner and outer shells. The effect of the shape, location and number of stiffeners on the axial and lateral behaviour of the columns is also one of the innovations of this study. The use of non-linear quasi-static analysis and finite element methods to accurately evaluate the axial and lateral performance of CFDST columns is one of the main objectives of this study.

2. Research Methods

2.1. Numerical modelling for verification

For verification, a numerical model must be created that matches the laboratory model, so in Abaqus software, all laboratory properties must be converted to a numerical model, and the laboratory results are obtained by compressing the numerical model, which will be discussed below. The design process in Abaqus software starts in the Parts module. This process involves three separate elements that are created in the Part module and then each element is assembled into its corresponding part in the Assembly module.

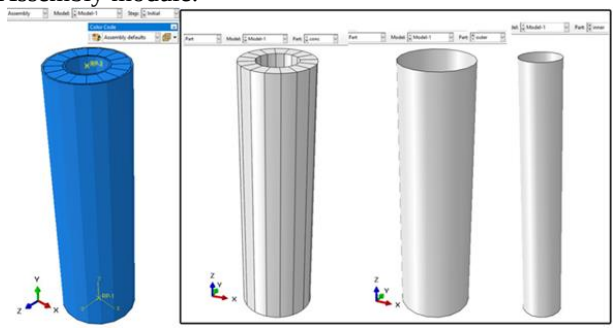

Figure 1 - In the Part module (right image) and the model assembly in the Assembly module (left image) of the Abaqus software.

Material properties in terms of shell thickness, steel yield stress and concrete strength between shells are created in the Material Properties module and assigned to the specimens (Figure 1). To solve the problem, the elements of the desired specimen should be divided into smaller sections in the Mesh module, so the optimum division rate of 5 mm was selected for each element, naturally the element type of the inner and outer shells is shell type and the concrete specimen is solid type. In order to apply the load and boundary conditions of the lower beam in the Interaction module of the Abaqus software, two reference points are created at the top and bottom of the specimen and a coupling constraint is created between these points (to facilitate the application of the load and boundary conditions of the beam). Also, in the same module, the direction of action and interaction of the space between the steel and concrete in the two shells should be defined by applying the coefficient of friction between the steel and concrete (of 0.30) and activating the surface interaction. To apply the load and support conditions in the Loading module of the Abaqus software, first define the gravity loading of the specimen and then fully constrain the lower coupler reference point in terms of displacement and rotation and load the upper coupler reference point (of the displacement control type) in increments of up to 20 mm (according to the laboratory specimen). After applying the load, to obtain the best and most accurate results, since the sample is under compressive load and there are buckling conditions in the steel section, one file should be run with buckling analysis and the other file with quasi-static analysis. These definitions are made in the STEP module of the Abaqus software. Therefore, in the first file, the sample is analysed under 9 buckling modes.

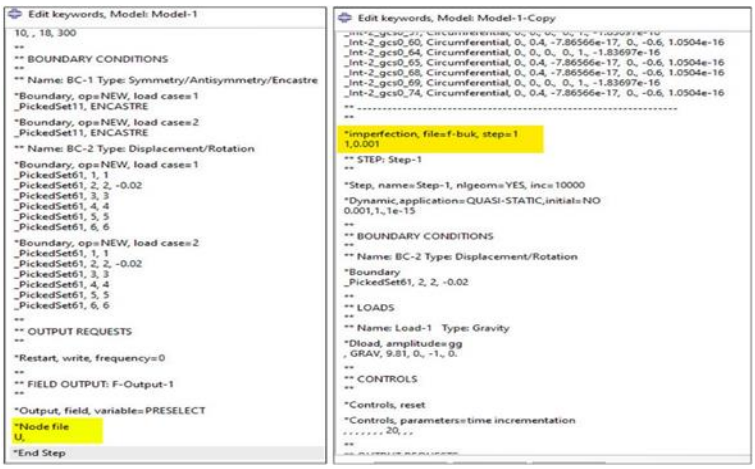

Figure 2 - Coding for transfer of displacement values from buckling analysis to quasi-static analysis.

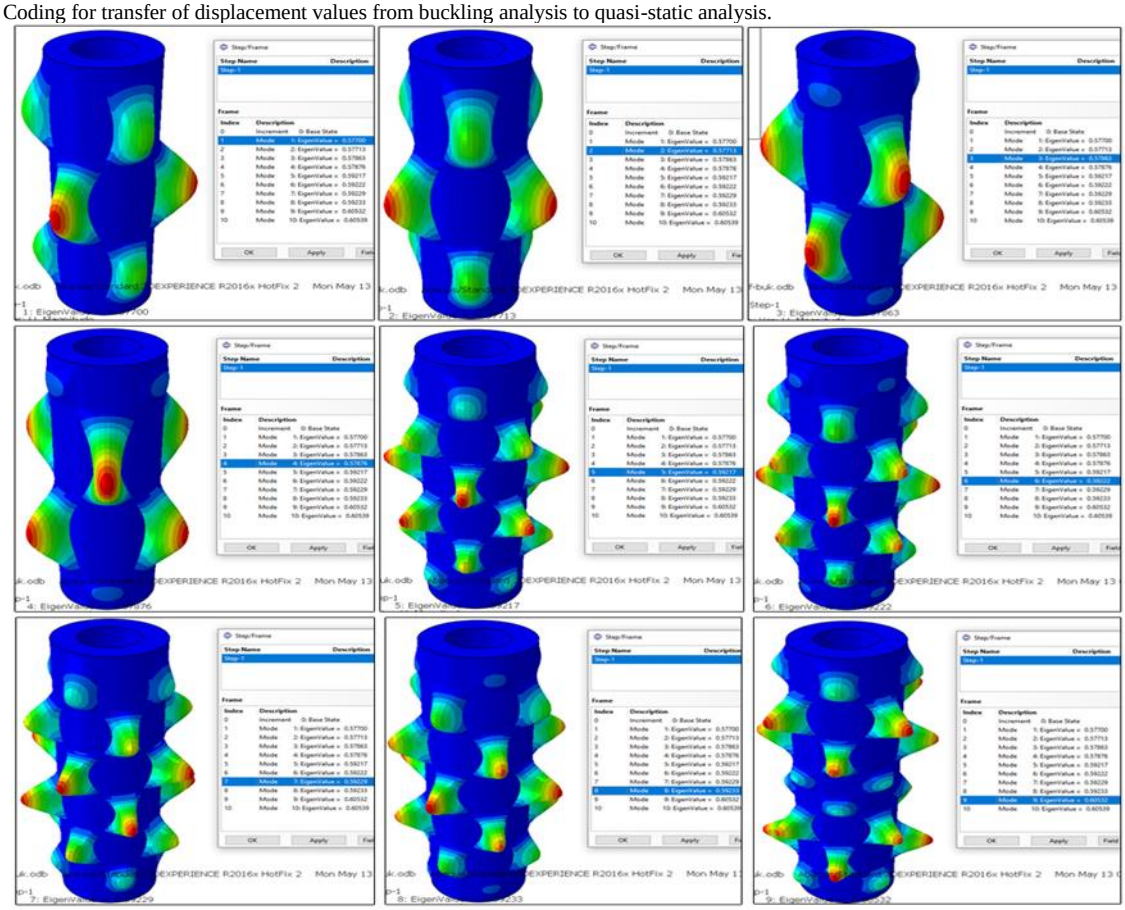

Figure 3 - Coding for transfer of displacement values from buckling analysis to quasi-static analysis

The deformation results of these buckling modes should be stored in a separate file and these results should be retrieved in the main quasi-static analysis file.

Meanwhile, the buckling modes of a double-shell steel column filled with prestressed concrete are shown in Figure 3.

After performing the above operations, the column specimen in question should be analysed using quasi-static analysis by applying compressive load, so by applying analysis in the work module, the results can be viewed in the results visualisation module. The results obtained after applying compressive loading show that compressive loading of the double-shell steel column specimen filled with concrete causes significant deformation in the outer and inner shell sections, as shown, and according to the same figure, the concrete has deformed more in the middle section. The results of the load-displacement and stress diagrams of the numerical specimen are also shown in

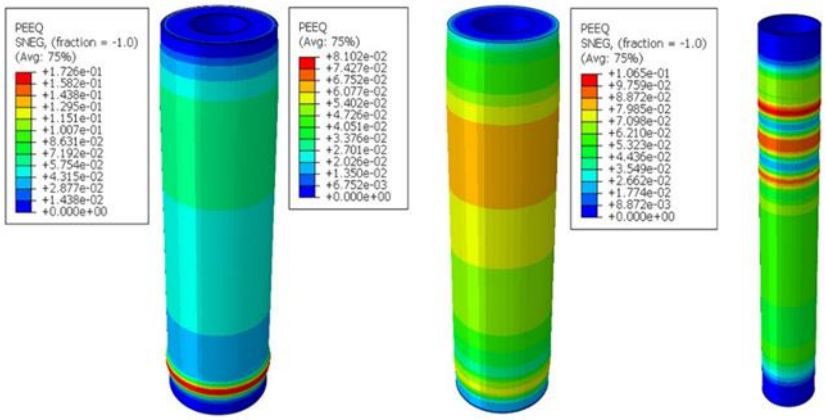

Figure 4 - Display of permanent deformation of concrete-filled double-shell steel column elements in relation to compressive loading in the results visualisation module of the Abaqus software.

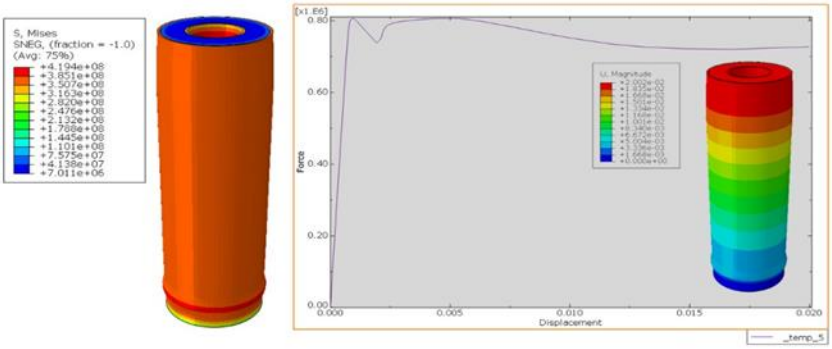

Figure 5 - Display of the von Mises stress of the specimen and the load-displacement diagram of the numerical specimen in the results visualisation module of the Abaqus software

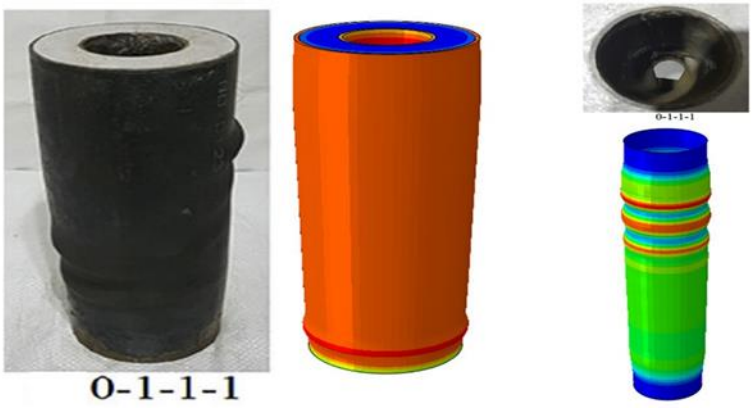

Figure 6 - Comparison and agreement of permanent deformation of specimens after completion of compressive loading between two numerical specimens and laboratory work (in specimen "0-1-1-1") Talha Akmakyapar et al

Figure 5.

2.2. Comparison and validation

In order to compare and validate the laboratory work of the concrete-filled double-shell steel column specimen (specimen "0-1-1-1") by Talha Ekmekiapar et al [11]. which was tested under quasi-static loading and additional axial (compressive) loading, and the numerical work, several parts of this comparison and validation should be carried out.

According to Figure 6, the permanent deformation of the specimen is observed in the two parts of the outer shell as a hump outward, i.e. the lower and middle parts upwards, as in the laboratory specimen, which is the same deformation observed in the numerical specimen. This outward hump is also observed in the inner shell between the two samples. Therefore, a shape match is observed between the two numerical and laboratory samples.

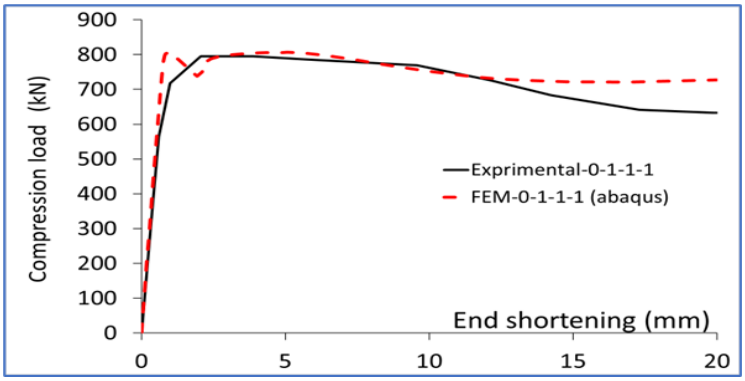

Figure 7 - Comparison and matching of load-displacement diagrams of specimens between two numerical specimens and laboratory work (in the "0-1-1-1" specimen) by Talha Ekmekiapar et al [11].

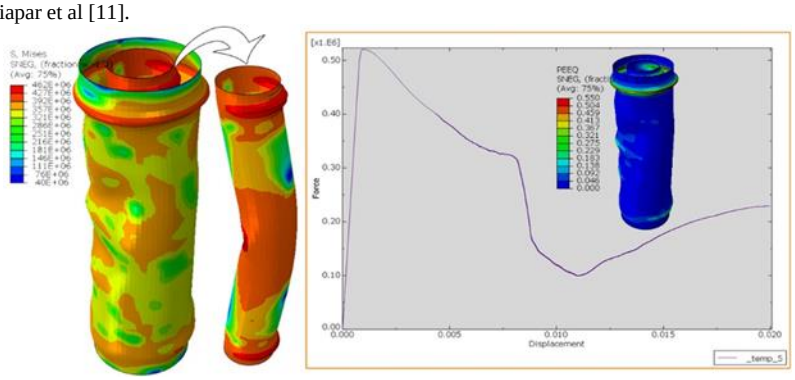

Figure 8 - Axial load results of a bare double shell steel column specimen without concrete and its axial load-displacement diagram in Abaqus software.

The second part of the comparison and matching can be done on the output results obtained from the experiment. The load-displacement diagram is the best option for this comparison and matching, so first the laboratory load-displacement diagram is converted to numerical data and then the diagram obtained from the Abaqus software is placed on top of it and the two are compared. Figure 7 shows the comparison between the two load-displacement diagrams of the laboratory and numerical samples.

According to Figure 7, as is also clear from the load-displacement diagram of the laboratory specimen, the maximum resistance of the "0-1-1-1" specimen is recorded at 790 kN, which is 800 kN for the numerical specimen, which is 1.2% of the difference in resistance criterion between the two specimens. In addition, the hardness of the specimen, which is the initial slope of the load-displacement diagram, is almost the same. According to the load-displacement diagram of the laboratory specimen, the hardness of the "0-1-1-1" specimen is 995 kN/mm, while the hardness of the numerical specimen is 1020 kN/mm, which is 2.9% of the difference in the hardness criterion between the two specimens. Also, in terms of the overall shape between the two laboratory and numerical diagrams, these two diagrams are almost the same, and the small difference may be due to various laboratory and numerical reasons.

Therefore, the two numerical and experimental models are in relatively good agreement and it can be said that the numerical model has been validated against the experimental model. Also, the studies in this part of the research can be used (both in terms of the Abaqus file and in terms of a reference model of a double-shell steel column filled with concrete) as the assumptions of section 3.

3. Analysis of the research results

Comparison of the axial and lateral performance of the base sample of a double-shell column without concrete with a double-shell column filled with concrete (between the two shells) In this part of the research, because there must be samples as a reference to compare the rest of the parametric samples with them, this part deals with the question of how much axial and lateral performance the base samples of the research have. The reference sample is the same sample that was tested in the third chapter, because the laboratory test results of this sample matched the numerical results, so the double-shell steel column filled with concrete is called "Ref", meaning the reference and base sample of this research. Another sample based on this research is a sample that is a double-shell steel column without concrete, and in order to be able to compare the

samples well, this sample is the same verified sample but without concrete between the two shells. Because the steel column is without concrete and bare, this column is introduced as "Bare".

The compressive (axial) loading results of the first sample "Ref" were presented in the second section, but the double shell steel column sample without concrete has not been loaded yet, so in the Abaqus software the results are obtained by copying the first file, removing the concrete and reloading the axial load. Figure 8 shows the axial load results of the double shell steel column without concrete. According to the result obtained from the load-displacement diagram of the concreteless double-shell steel column sample in Figure 8, the concreteless double-shell steel column reaches the axial yield point and buckles when subjected to a compressive load with an axial displacement of about 1 mm and an axial resistance of 521 kN. The von Mises stress and deformation of the sample in both the inner and outer shells are shown in Figure 8.

As mentioned above, the "Bare" specimen is identical to the "Ref" specimen in all dimensional and material properties, except that in the "Bare" specimen there is no concrete between the two shells. By plotting the results of the reference samples in the form of a load-displacement diagram, we can comment on the results obtained. Figure 9 shows the axial load-displacement diagram of the two reference specimens. As can be seen from Figure 9, the double-shell steel column without concrete, because it does not have a concrete column in its body and because of the buckling of the steel body in the inner and outer shells, buckles earlier and has a lower compressive performance than the double-shell steel column filled with concrete. These functions are clearly visible in the initial slope of the load-displacement diagram (representing the initial axial stiffness of the specimens) and the maximum axial strength (representing the axial strength criterion). Also, in the load-displacement diagram and axial loading of the specimens, the curve of the diagram changes slope (stiffness) at the yield point and the specimens only deforms. According to Figure 9, in the sample of double-shell steel column filled with concrete, after the yield point, the resistance diagram remains almost constant, slightly less than the maximum resistance, but in the double-shell steel column without concrete, the resistance decreases sharply and becomes a decrease, which is a phenomenon in the ductility criterion.

By bilinearising the load-displacement diagram with the equivalent energy model, multi-line diagrams are transformed into just two lines and these two lines represent the diagram so that the area lost and the area gained are equal in the resulting diagram. By bilinearising the load-displacement diagram, the yield point of the diagrams can be calculated and with the yield point the axial power can be calculated and compared. Therefore, according to Figure 10, the graphs become two lines and

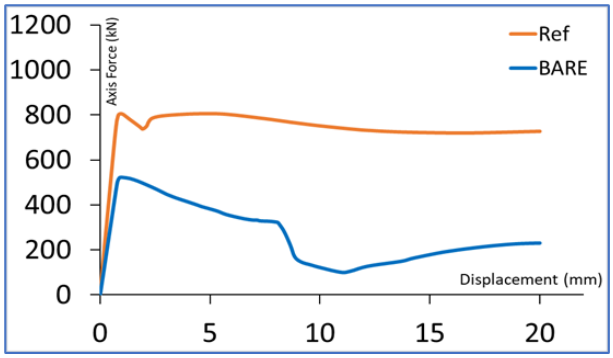

Figure 9 - Comparison of the axial load-displacement diagram of the "Ref" concrete-filled and the "Bare" concrete-free double-shell steel column specimens

according to this figure, all the information of the yield point, the performance endpoints and the maximum recorded resistance is shown. According to Figure 10, the axial performance endpoint of the "Bare" specimen occurs at a displacement of 4.6 mm and, due to the compressive buckling of the column without concrete, the continuation of its axial load-displacement diagram is not part of the axial performance, whereas in the "Ref" specimen, due to the presence of concrete in the column, the entire load length, i.e. 20 mm, is considered part of the performance. This is taken into account in the calculation of the axial ductility and it is obvious that the ductility of the specimen with concrete is much higher than that of the column without concrete.

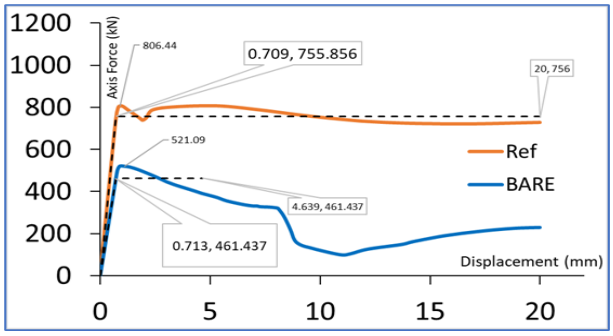

Figure 10 - Comparison of the two-line load-axial displacement diagram data of the "Ref" concrete-filled double-shell steel column and the "Bare" concrete-free double-shell steel column

Table 1 shows the comparison of axial performance between two concrete filled double shell steel column base specimens "Ref" and a concrete free double shell steel column specimen "Bare".

According to Table 1, the yield point in the displacement section of the concrete-filled double-shell steel column "Ref" specimen is only 1% lower than the same case of the concrete-free double-shell steel column "Bare" specimen, but its yield point load is 64% higher, so the slope (stiffness) of the load-displacement diagram should also be higher. Similarly, the axial stiffness of the

"Ref" specimen is 65% higher than that of the "Bare" specimen. According to the table, the ultimate displacement yield point of the "Bare" specimen occurs earlier and the ductility, which is the result of dividing the ultimate displacement yield point by the yield displacement yield point, should be lower. For example, the axial ductility of the "Bare" sample is 6.5 and the axial ductility of the "Ref" sample is 28.2, which is more than 3 times. In terms of strength, the strength of the "Ref" sample is 55% higher than that of the "Bare" sample. It is therefore clear how its axial performance is increased by filling the space between the two shells with concrete.

Table 1
Comparative axial performance data between the two baseline samples 'Ref' and 'Bare'.

Spectrum	Δy (mm)	V_y (kN)	Δu (mm)	P_{sh} (kN)	K_{sh} (kN/mm)	μ_{sh}
Ref	0.709	756	20	806	1066	28.20
Bare	0.713	461	4.64	521	647	6.50
	-1%	64%	331%	55%	65%	334%

In the case of lateral loading in two specimens, a double-skinned steel column filled with concrete "Ref" and a double-skinned steel column without concrete "Bare", all features of the application of software properties (except the loading path) are fixed. In this way, the load path is applied laterally to the specimens instead of axially as a displacement control. First, the double-shell steel column specimen filled with concrete "Ref" and then the double-shell steel column specimen without concrete "Bare" are subjected to lateral loading, and the results of applying lateral loading are shown in Figures 11 and 12, respectively.

The von Mises stress and deformation of the specimen in both the inner and outer shells are known for both the concrete-filled double-shell steel column "Ref" and the concrete-free double-shell steel column "Bare". Also, by bilinearising the lateral load-displacement diagram, the yield point of the diagrams can be calculated, and with the yield point, the lateral performance can be calculated and compared. Therefore, Figure 13 shows the yield points of the diagrams side by side and compares them.

Table 2 shows the comparison of lateral performance between two concrete filled double shell steel column base specimens "Ref" and a concrete free double shell steel column specimen "Bare".

According to Table 2, the lateral strength criterion of the "Ref" concrete-filled double-shell steel column base specimen is 19% higher than that of the "Bare" concrete-free double-shell steel column base specimen. Also, the lateral initial stiffness criterion of the concrete-filled double-shell steel column base specimen "Ref" is 39% higher than that of the concrete-free double-shell steel column specimen "Bare", and the lateral ductility criterion of the concrete-filled double-shell steel column base specimen "Ref" is 14% higher than that of the concrete-free double-shell steel column specimen "Bare". It is therefore clear how the lateral performance is increased by filling the space between the two shells with concrete.

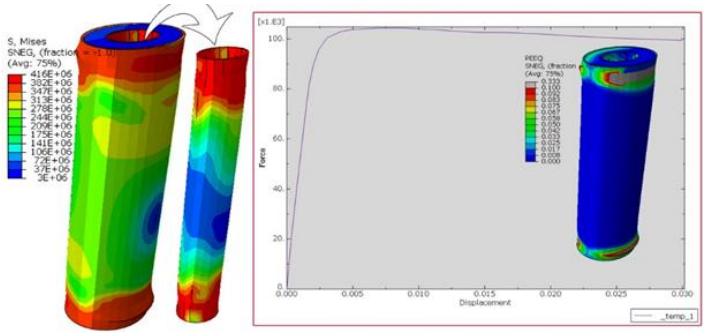

Figure 11 - Lateral loading results of concrete filled steel column "Ref" sample and its lateral load-displacement diagram

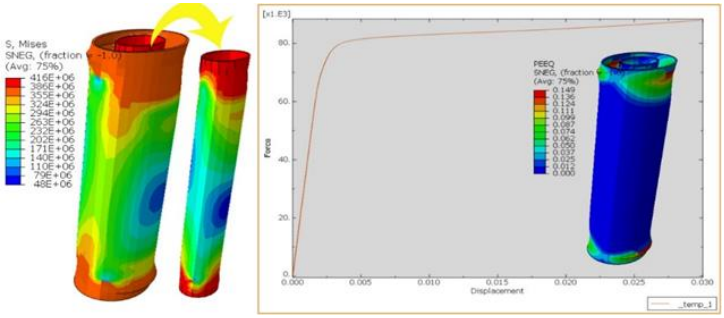

Figure 12 - Results of the lateral loading of a double-shell steel column with no 'bare' concrete and the lateral load-displacement diagram

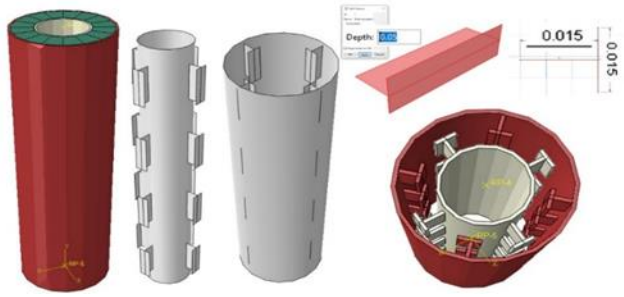

Figure 14 - Example of a double shell steel column filled with concrete with a T-shaped stiffener, section at 4 parts of the column height (example "T8-4").

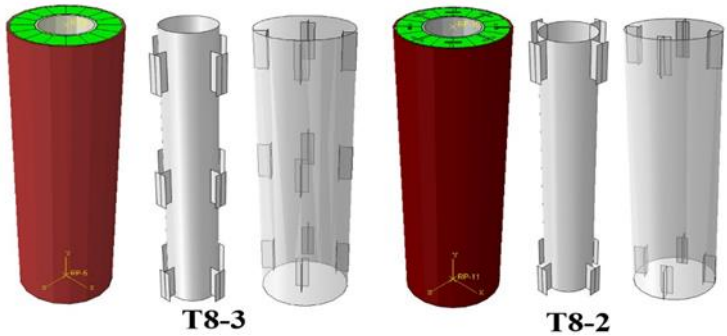

Figure 15 - Examples of double shell steel columns filled with concrete with T-shaped stiffeners at 3 and 2 parts of the column height (examples "T8-3" and "T8-2").

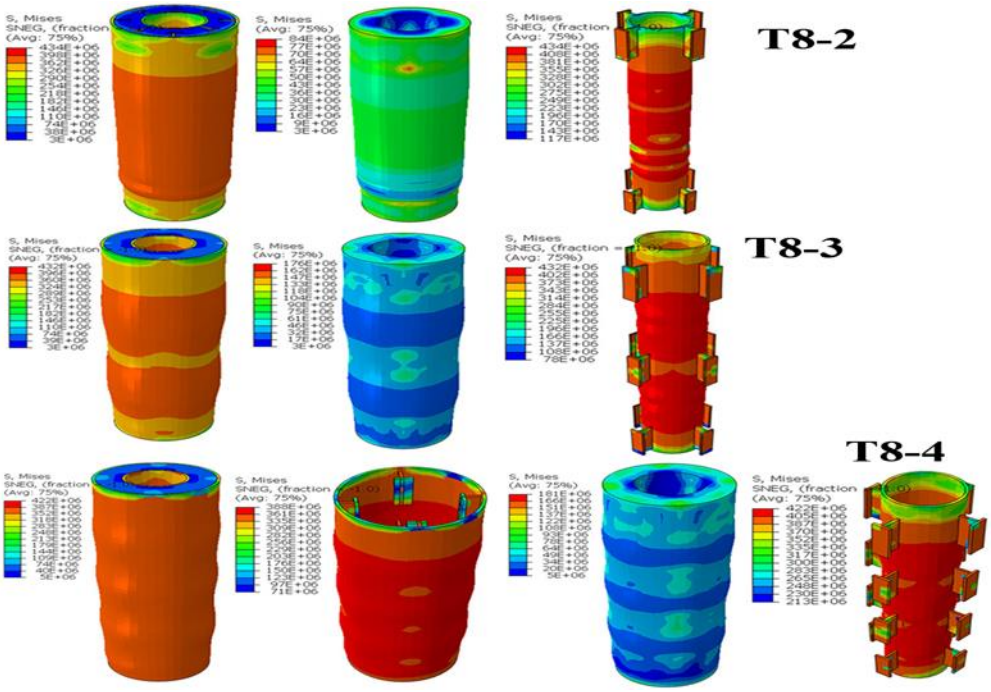

Figure 16 - Axial loading results - von Mises stress in concrete filled double shell steel column specimens with T-shaped section stiffeners at 2, 3 and 4 parts of column height (specimens "T8-2", "T8-3" and "T8-4").

3.1. Comparison of the axial behaviour of concrete-filled double-shell columns with a T-shaped stiffener in the cross-section and with a global T-shaped stiffener

In this part of the research, the problem is addressed: if steel stiffeners are used in the space between the two shells, how will the axial performance factors of a double-shell steel column filled with concrete change? Therefore, a T-section stiffener is proposed, modelled with a flange and web of 1.5 cm, a height of 5 cm and a thickness of 2.7 mm. Four of them are welded to the inner shell and the other four to the outer shell. During installation, they are placed

at a 45-degree angle to each other so that they do not collide. Finally, the space between the stiffeners is filled with concrete. In Figure 4-8, these stiffeners are placed at 4 different heights in the column. This column has a total of 8 T-shaped stiffeners in the radial direction. The name "T8-4" has been considered for this example, which is located at 4 column heights with 8 T-shaped stiffeners.

The fact that the cross-sectional stiffeners are located at 3 and 2 parts of the column height has resulted in the steel column specimens "T8-3" and "T8-2" shown in Figure 15.

The results of the axial loading of the three new specimens in terms of von Mises stress and the results of the force-displacement diagram are shown in Figures 16 and 17 respectively.

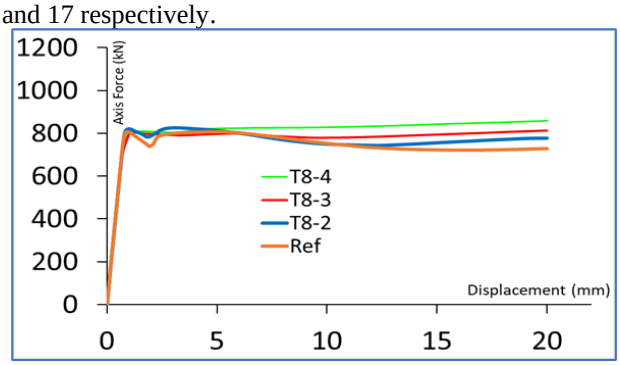

Figure 17 - Comparison of axial load-displacement diagrams of a concrete filled double shell steel column specimen with T-shaped section stiffeners at 2, 3 and 4 parts of the column height (specimens "T8-2" and "T8-3" and "T8-4").

According to Figure 16, the von Mises stress of the concrete-filled double-shell steel column specimens with T-shaped sectional stiffeners at 2, 3 and 4 parts of the column height (specimens "T8-2" and "T8-3" and "T8-4") is shown in accordance with the axial loading results. Figure 17 shows that the stress in the inner shell is higher than the rest of the parts and the type of stiffener is effective in the deformations caused by axial loading. Figure 17 also shows that the specimens with sectional reinforcement with T-shaped stiffeners have a slight increase in ultimate strength compared to the reference specimen "Ref", so that as the number of stiffeners in height increases, the ultimate strength also increases. For a better comparison between the results of the specimens studied, their axial performance is also calculated by bilinearising the load-displacement diagram, the results of which are shown in Table 3.

According to Table 3, the column strength criterion increases as the number of stiffeners in the column height increases, so that this increase is 2.5, 1 and 6.5% for samples "T8-2", "T8-3" and "T8-4" respectively.

In this part of the research, the question is: if a global steel stiffener is used in the space between the two shells instead of a sectional steel stiffener, what is the change in the axial performance factors of a double-shell steel column filled with concrete? Therefore, the same stiffener is modelled according to Figure 18 with a height equal to the height of the column, so that these columns are named according to the number of T-shaped stiffeners.

Table 3 - Comparison of axial performance data between concrete filled double shell steel column specimens with T-shaped section stiffeners at 2, 3 and 4 parts of the column height (specimens "T8-2" and "T8-3" and "T8-4")

Spectrum	Δy (mm)	Vy (kN)	Δu (mm)	Psh (kN)	Ksh (kN/mm)	μax
Ref	0.709	756	20	806	1066	28.20
T8-2	0.735	776	20	826	1056	27.22
T8-3	0.747	794	20	814	1063	26.77
T8-4	0.775	831	20	859	1072	25.82

According to Figure 18, the double shell steel columns filled with concrete with T-shaped global stiffeners, which have 2 stiffeners in the inner shell and 2 stiffeners in the outer shell, have a total of 4 T-shaped global stiffeners, named "T4", and similarly, the "T6" and "T8" specimens have 6 and 8 T-shaped global stiffeners, respectively. Figure 19 shows the von Mises stress results of the specimens.

Figure 19 shows that the stress in the inner shell is higher than the rest of the outer shell and that the type of stiffener is effective in the deformations caused by the axial load, so that in sample "T4" the column has deformed in the upper part of the outer shell. Figure 20 shows the results of the force-displacement diagram.

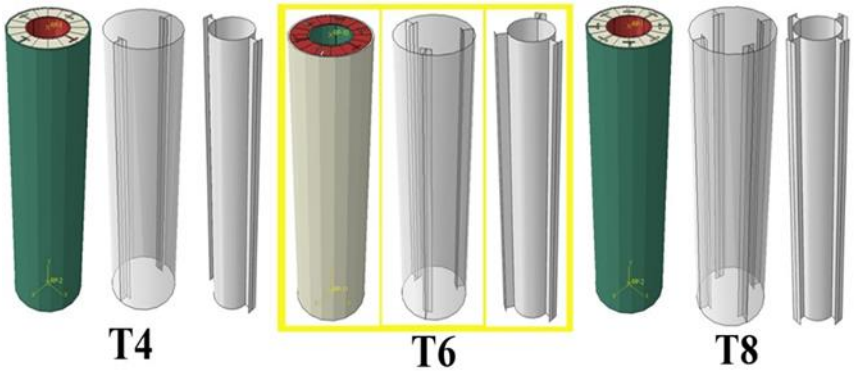

Figure 18 - Examples of concrete filled double shell steel columns with continuous T-shaped stiffeners (examples "T4", "T6" and "T8").

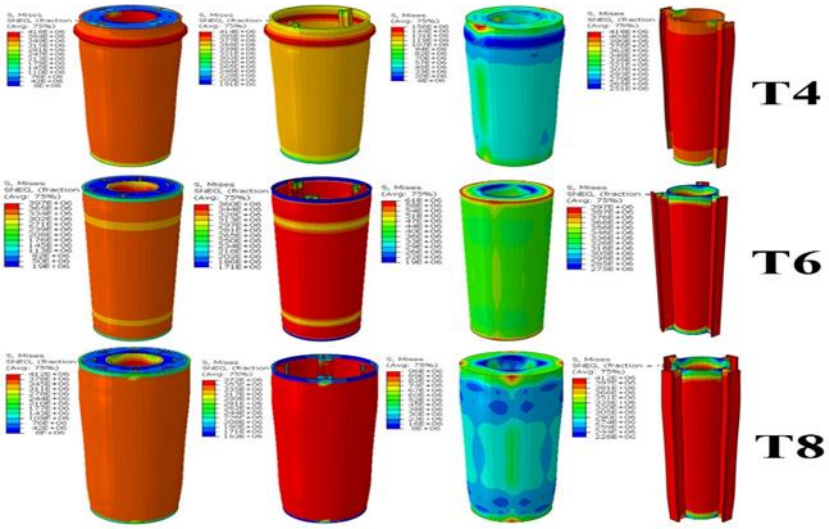

Figure 19 - Axial load results - von Mises stress in concrete filled double shell steel column specimens with global T-shaped stiffeners (specimens "T4", "T6" and "T8").

For a better comparison between the results of the specimens studied, their axial performance is also calculated by bilinearising the load-displacement diagram, the results of which are shown in Table 4.

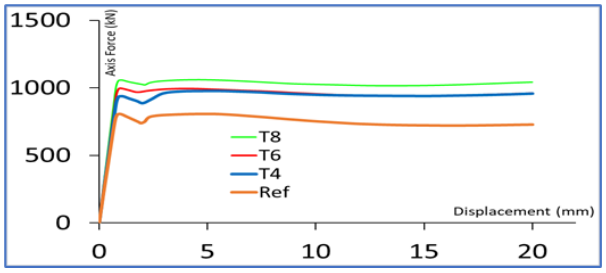

Figure 20 - Comparison of axial load-displacement diagrams of concrete filled double shell steel column specimens with global T-shaped stiffeners (specimens "T4", "T6" and "T8").

Table 4

Comparison of axial performance data between concrete filled double shell steel column specimens with global T-shaped stiffeners (specimens "T4", "T6" and "T8").

Spectrum	Δy (mm)	Vy (kN)	Δu (mm)	Psh (kN)	Ksh (kN/mm)	μax
Ref	0.709	756	20	806	1066	18.20
T4	0.823	950	20	977	1155	24.31
T6	0.785	964	20	997	1227	25.47
T8	0.797	1034	20	1060	1298	25.11

According to Table 4, as the number of T-shaped stiffeners in the column increases, the axial stiffness criterion of the column increases, so that this increase is 21, 24 and 31% for samples "T4", "T6" and "T8" respectively. Table 4 also shows that as the number of T-shaped stiffeners in the column increases, the axial stiffness criterion of the column increases, so that this increase is 8, 15 and 22% for samples "T4", "T6" and "T8" respectively. However, as far as the ductility of the column is concerned, as the number of stiffeners in the height of the column increases, the axial ductility criterion decreases, so that for samples "T4", "T6" and "T8" it decreases by 14, 10 and 11% respectively. Now, if the results of the total axial performance information of the samples with cross-sectional and global T-shaped stiffeners are placed side by side, this can be discussed, so this comparison is made in Table 5.

Table 5 - Comparison of the axial performance data between the concrete filled double shell steel column specimens with a T-shaped cross-section and with global stiffeners

Spectrum	Δy (mm)	Vy (kN)	Δu (mm)	Psh (kN)	Ksh (kN/mm)	μax
T8	0.797	1034	20	1060	1298	25.11
T6	0.785	964	20	997	1227	25.47
T4	0.823	950	20	977	1155	24.31
T8-4	0.775	831	20	859	1072	25.82
T8-2	0.735	776	20	826	1056	27.22
T8-3	0.747	795	20	814	1063	26.77
Ref	0.709	756	20	806	1066	18.20

According to Table 5, the concrete-filled double-shell steel column specimens with T-shaped global stiffeners have higher strength and stiffness criteria than the concrete-filled double-shell steel column specimens with T-shaped cross-sectional stiffeners due to the direct participation of the stiffeners in axial load transfer. Also, the number of T-shaped stiffeners in both cross-sectional and global specimens has a direct relationship in increasing the axial strength and stiffness criteria. Figure 21 also shows the performance of each specimen divided by the performance of the base specimen and its details.

According to Figure 21, by comparing the relative performance of the concrete-filled double-shell steel column specimens with T-shaped cross-sectional and global stiffeners with the base specimen, it can be

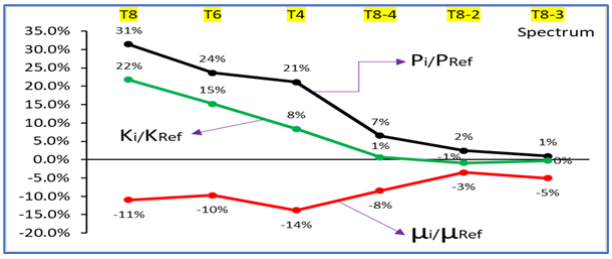

Figure 21 - Comparison of the relative performance of concrete filled double shell steel column specimens with sectional and global T-stiffeners compared to the base specimen

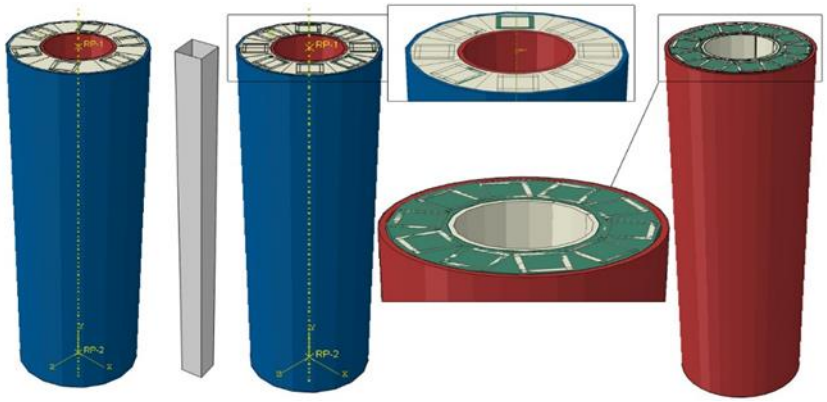

Figure 22 - Example of a double shell steel column filled with concrete with a continuous square stiffener (examples "Box6", "Box8" and "Box10")

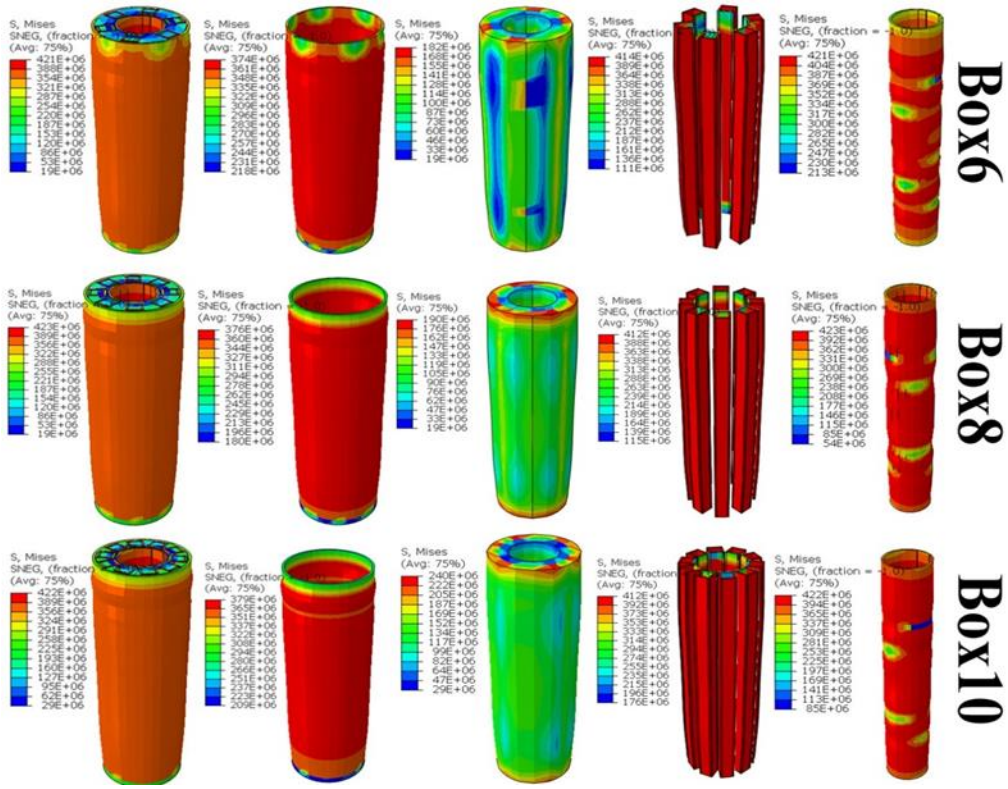

Figure 23 - Axial load results - von Mises stress in concrete filled double shell steel column specimens with square stiffeners throughout (examples "Box6", "Box8" and "Box10").

concluded that the concrete-filled double-shell steel column specimens with T-shaped cross-sectional stiffeners do not have very high axial performance, but the concrete-filled double-shell steel column specimens with T-shaped global stiffeners have higher axial performance.

3.2. Comparison of axial behaviour of concrete filled double shelled columns and square stiffening

This part of the research deals with the question of how the axial performance factors of a double-shell steel column filled with concrete change when a square steel stiffener is used in the space between the two shells. Therefore, a square stiffener is proposed that is considered without welding to the shells and only by placing it inside the shells and then pouring concrete in the space between the two concrete shells. These stiffeners have dimensions of 2 x 2 cm and a height of 40 cm. These columns have a total of 6, 8 and 10 square stiffeners in the radial direction, called "Box6", "Box8" and "Box10" respectively. Obviously, the criteria for the number of these stiffeners are the same for all stiffeners, namely 6 and 8, and the number 10 is used because more than 10 square stiffeners cannot fit into this column and will collide with each other (Figure 22).

Figure 23 shows the von Mises stress results for the specimens investigated. It shows that the highest stresses are in the outer shell, followed by the square stiffeners and then the outer shell. Figure 24 also shows the results of the force-displacement diagram. For a better comparison between the results of the specimens studied, their axial performance is also calculated by bilinearising the load-displacement diagram, the results of which are shown in Table 6.

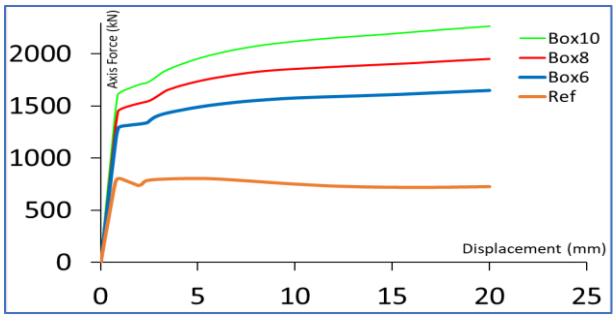

Figure 24 - Comparison of axial load-displacement diagrams of concrete filled double shell steel column specimens with continuous square stiffeners (specimens "Box6", "Box8" and "Box10").

Table 6
Comparison of axial performance data between concrete filled double shell steel column specimens with universal square stiffeners ("Box6", "Box8" and "Box10" specimens).

Spectrum	Δy (mm)	Vy (kN)	Δu (mm)	Psh (kN)	Ksh (kN/mm)	μax
Ref	0.709	759	20	806	1066	28.20
Box6	0.999	1547	20	1651	1549	20.02
Box8	1.049	1813	20	1729	1729	19.07
Box10	1.084	2072	20	1911	1911	18.45

According to Table 6, as the number of square stiffeners in the column increases, the axial stiffness criterion of the column increases so that this increase is 105, 142 and 181% for samples "Box6", "Box8" and "Box10" respectively. Table 6 also shows that as the number of square stiffeners in the column increases, the axial stiffness criterion of the column increases, so that this increase is 45, 62 and 79% for the "Box6", "Box8" and "Box10" samples respectively. However, as far as the ductility of the column is concerned, the axial ductility criterion decreases as the number of stiffeners increases, so that it decreases by 29, 32 and 35% respectively for samples "Box6", "Box8" and "Box10".

3.3. Comparison of axial performance of concrete-filled double-shell columns and circular stiffeners

This part of the research is concerned with how the axial performance factors of a concrete-filled double-shell steel column change when a circular steel stiffener is used in the space between the two shells. Therefore, a circular stiffener is proposed that is not welded to the shells, but is simply placed inside the shells and then concrete is poured into the space between the two concrete shells. These stiffeners have a diameter of 2.35 cm and a height of 40 cm. These columns have a total of 6, 8 and 11 circular stiffeners in the radial direction, named "Cir6", "Cir8" and "Cir11" respectively. Obviously, as far as the number of these stiffeners is concerned, the criteria of the two numbers 6 and 8 are constant for all stiffeners and the number 11 is used because more than 11 circular stiffeners cannot fit into this column and they will collide with each other (Figure 25).

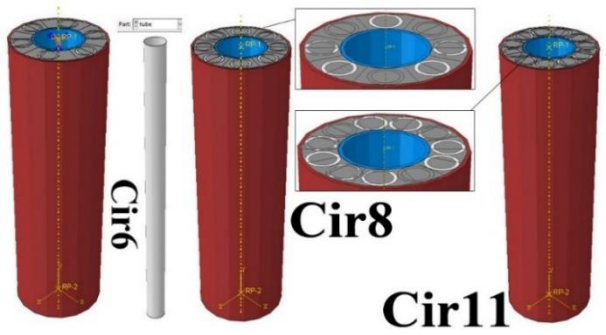

Figure 25 - Example of a concrete filled double shell steel column with global circular stiffener (examples "Cir6", "Cir8" and "Cir11").

Figure 26 shows the von Mises stress results for the specimens investigated. It shows that the highest stresses are in the outer shell, followed by the circular stiffeners and then the outer shell. Figure 27 also shows the results of the force-displacement diagram. For a better comparison between the results of the specimens studied, the axial performance is also calculated by bilinearising the load-displacement diagram, the results of which are shown in Table 7.

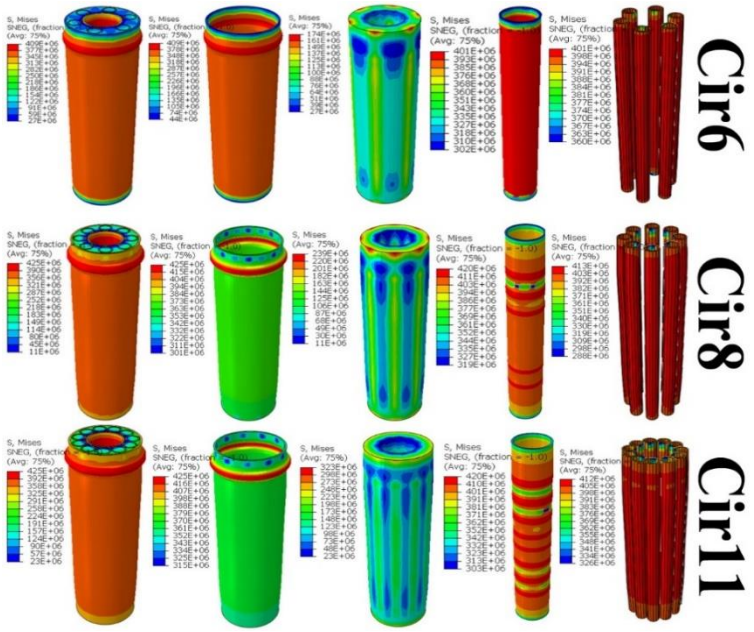

Figure 26 - Axial loading results - von Mises stress in concrete filled double shell steel column specimens with global circular stiffeners (specimens "Cir6", "Cir8" and "Cir11").

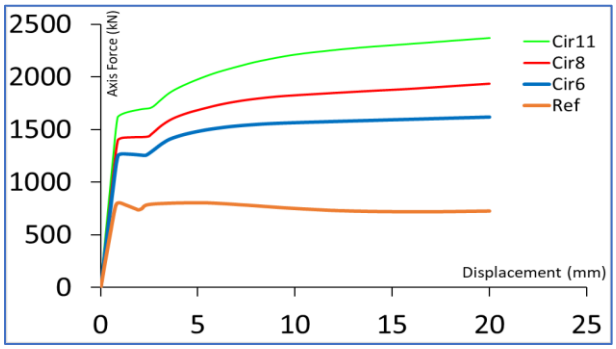

Figure 27 - Comparison of axial load-displacement diagrams of concrete filled double shell steel column specimens with global circular stiffeners (specimens "Cir6", "Cir8" and "Cir11")

Table 7
Comparison of axial performance data between concrete filled double shell steel column specimens with global circular stiffeners (specimens "Cir6", "Cir8" and "Cir11").

Spectrum	Δy (mm)	Vy (kN)	Δu (mm)	Psh (kN)	Ksh (kN/mm)	μax
Ref	0.709	759	20	806	1066	28.20
Cir6	1.013	1527	20	1620	1507	19.75
Cir8	1.061	1775	20	1973	1673	18.85
Cir11	1.116	2144	20	1922	1922	1793

According to Table 7, as the number of global circular stiffeners in the column increases, the axial stiffness criterion of the column increases so that this increase is 101, 140 and 194% for samples "Cir6", "Cir8" and "Cir11" respectively. Table 7 also shows that as the number of global circular stiffeners in the column increases, the axial stiffness criterion of the column also increases, so that this increase is 41, 57 and 80% for samples "Cir6", "Cir8" and "Cir11" respectively. However, as far as the ductility of the column is concerned, the axial ductility criterion decreases as the number of stiffeners increases, so that for samples "Cir6", "Cir8" and "Cir11" it decreases by 30, 33 and 36% respectively.

3.4. Comparison of axial performance of concrete-filled double-shell columns and trapezoidal stiffeners

This part of the research deals with the question of how the axial performance factors of a concrete-filled double-shell steel column change when a global trapezoidal steel stiffener is used in the space between the two shells. Therefore, the global trapezoidal stiffener is recommended due to its suitable dimensional adaptation to the space between the two shells, which is considered without welding to the shells and only by placing it inside the shells and then pouring concrete in the space between the two concrete shells. These stiffeners have a trapezoidal base width of 1.24 and 2 cm, a trapezoidal base height of 2 cm and a column height of 40 cm. These columns have a total of 6, 8 and 16 trapezoidal stiffeners in the radial direction, designated "Tra6", "Tra8" and "Tra16" respectively. Obviously, as far as the number of these stiffeners is concerned, the criteria of the two numbers 6 and 8 are constant for all the stiffeners, and the number 16 is also used because 16 trapezoidal stiffeners are placed inside this column in such a way as to include the entire capacity of the stiffeners without the sections colliding. It is explained that this number of stiffeners (16) is the maximum number

of stiffeners that could be placed in the space between the two shells because the trapezoidal shape has a suitable dimensional fit for the space between the two shells (Figure 28). Figure 29 also shows the results of the force-displacement diagram. In order to better compare the results of the specimens studied, their axial performance is also calculated by bilinearising the force-displacement diagram, the results of which are shown in Table 8.

According to Table 8, as the number of trapezoidal stiffeners in the column increases, the axial stiffness criterion of the column increases, so that this increase is 86, 120 and 250% for samples "Tra6", "Tra8" and "Tra16" respectively. Table 8 also shows that as the number of trapezoidal stiffeners in the column increases, the axial stiffness criterion of the column also increases, so that this increase is 41, 56 and 119% for samples "Tra6", "Tra8" and "Tra16" respectively. On the other hand, as far as the ductility of the column is concerned, the axial ductility criterion decreases as the number of stiffeners increases, so that it decreases by 25, 29 and 35% respectively for samples "Tra6", "Tra8" and "Tra16".

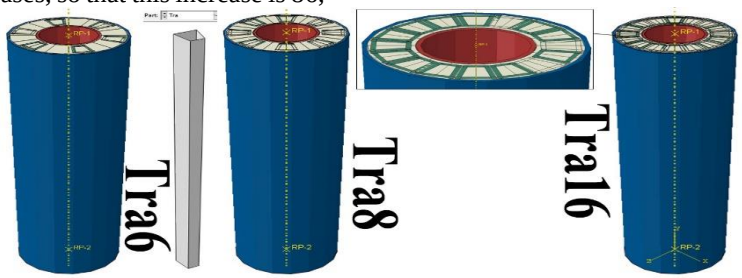

Figure 28- Example of concrete filled double shell column with trapezoidal stiffener (examples "Tra6", "Tra8" and "Tra16")

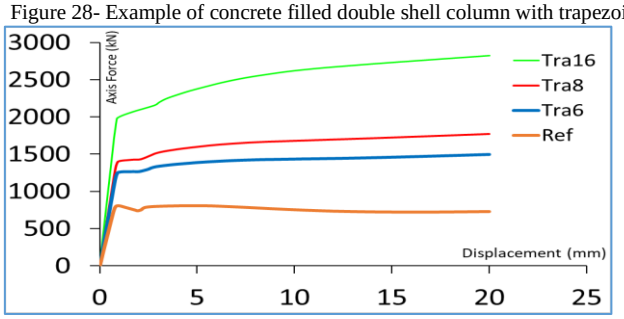

Figure 29 - Comparison of axial load-displacement diagrams of concrete filled double shell steel column specimens with continuous trapezoidal stiffeners (specimens "Tra6", "Tra8" and "Tra16")

Table 8 - Comparison of axial performance data between concrete filled double shell steel column specimens with continuous trapezoidal stiffeners (specimens "Tra6", "Tra8" and "Tra16").

Spectrum	Δy (mm)	Vy (kN)	Δu (mm)	Psh (kN)	Ksh kN/mm	Max
Ref	0.709	759	20	806	1066	28.20
Cir6	1.013	١٤٢٠	20	١٤٩٧	١٥٠٣	٢١,١٦
Cir8	1.061	١٦٥٩	20	١٧٧٤	١٦٦٧	٢٠,١٦
Cir16	1.116	٢٥٦٠	20	٢٨٢٤	٢٣٣٣	١٨,٢٣

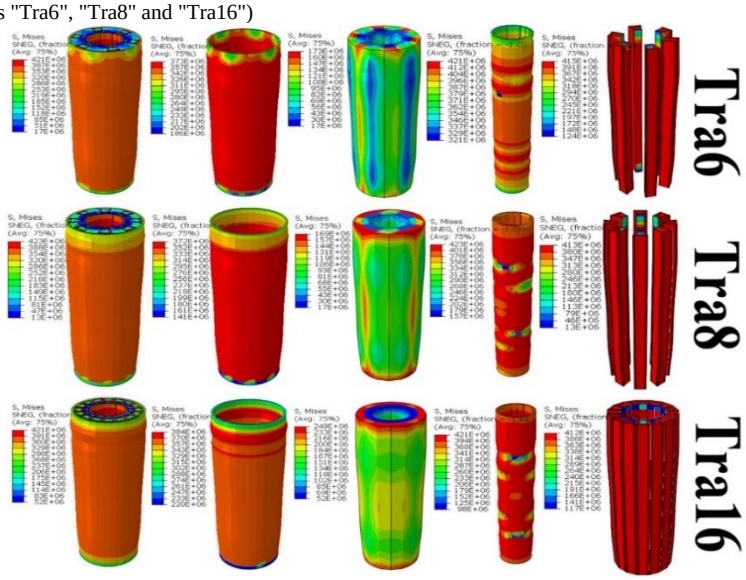

Figure 30 - Axial load results - von Mises stress in concrete filled double shell steel column specimens with continuous trapezoidal stiffeners (specimens "Tra6", "Tra8" and "Tra16").

3.5. Comparison of axial performance of concrete-filled double-shell columns and square, circular and trapezoidal stiffeners

T-shaped stiffeners were used as stiffeners in concrete-filled double-shell columns, which had to be welded to the inner or outer shell, but stiffeners such as square, circular and trapezoidal stiffeners are placed without welding only in the space between the two shells and then concrete is poured in the space between the two shells. In the previous sections, the axial performance comparison was made between concrete-filled double-shell columns with T-shaped stiffeners, but here the axial performance comparison is made between concrete-filled double-shell columns and square, circular and trapezoidal stiffeners. To begin the comparison, the force-displacement diagrams of three concrete-filled double-shell columns with square, circular and trapezoidal stiffeners with 8 stiffeners are compared side by side in Figure 31. According to Figure 31, the three samples of concrete-filled double-shell columns with square, circular and trapezoidal stiffeners with 8 stiffeners behave almost the same, with the difference that the concrete-filled double-shell column sample with 8 trapezoidal stiffeners has a lower axial performance in strength and stiffness than the square and circular samples, then the circular sample and finally the square sample have higher performances. It seems that if the force-displacement diagram of all the concrete-filled double-shell column samples with square, circular and trapezoidal stiffeners is compared side by side, the comparison of the samples will be clearer. This is therefore shown in Figure 4-26. In addition, Table 9 shows the side-by-side comparison of the axial performance data of the concrete-filled double-shell steel column specimens with square, circular and trapezoidal stiffeners.

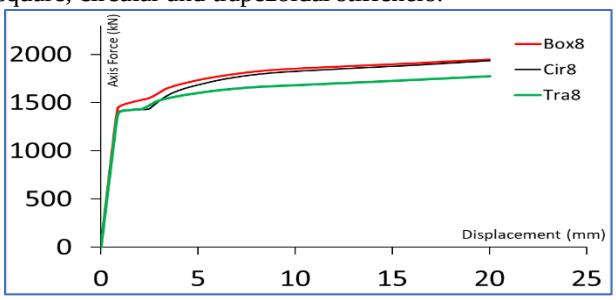

Figure 31 - Comparison of axial load-displacement diagram of concrete filled double shell column with square, circular and trapezoidal stiffeners for a total of 8 stiffeners

According to Table 9, the concrete-filled double-shell steel column specimen with 16-foot trapezoidal stiffener has a higher strength and stiffness criterion due to the direct involvement of the stiffeners in the axial load transfer, followed by the concrete-filled double-shell steel column specimen with 11-foot circular stiffener and the concrete-filled double-shell steel column specimen with 10-foot square stiffener. This shows that the shape of the internal stiffener section, where appropriate, allows a greater number of that section to fit inside the column and increases performance. In other cases, where the maximum number is not taken into account, these are square, circular and trapezoidal sections respectively. Figure 33 also divides the performance of each sample by the performance of the base sample and shows its details.

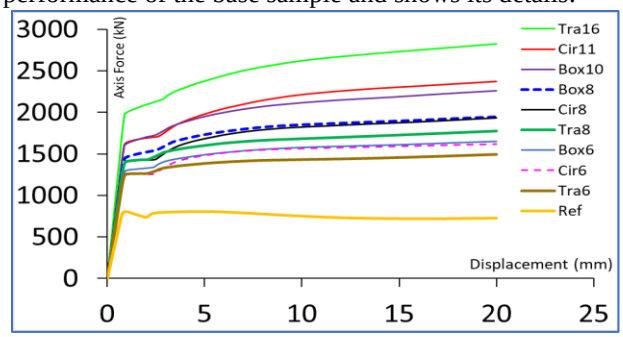

Figure 32 - Comparison of axial load-displacement diagrams of all concrete filled double shell steel column specimens with square, circular and trapezoidal stiffeners

Table 9

Comparison of the axial performance data of all the concrete filled double shell steel column specimens with square stiffeners, circular stiffeners and trapezoidal stiffeners.

Spectrum	Δy (mm)	Vy (kN)	Δu (mm)	Psh (kN)	Ksh (kN/mm)	μax
Tar16	1.097	2560	20	2824	2333	18.23
Cir11	1.116	2144	20	2372	1922	17.93
Box10	1.084	2072	20	2264	1911	18.45
Cir8	1.049	1813	20	1950	1729	19.07
Box8	1.061	1775	20	1934	1673	18.85
Tra8	0.995	1659	20	1774	1667	20.10
Cir6	0.999	1547	20	1651	1549	20.02
Box6	1.013	1527	20	1620	1507	19.75
Tra6	0.945	1420	20	1497	1503	21.16
Ref	0.709	756	20	806	1066	28.20

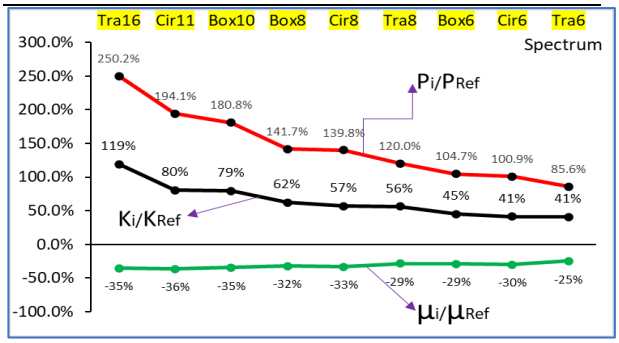

Figure 33 - Comparison of relative performance of concrete filled double shell steel column specimens with square, circular and trapezoidal stiffeners against the base specimen

From Figure 33, comparing the relative performance of the concrete filled double shell steel column specimens with square, circular and trapezoidal stiffeners compared to the base specimen, it can be concluded that the number of stiffeners has a direct relationship with the axial performance and that the shape of the stiffener also affects the axial performance of the specimens.

3.6. Investigation of lateral performance, double-shell column filled with concrete and types of stiffeners

In this part of the research, assuming that all the characteristics of the model, including the software characteristics, remain constant, the problem is addressed: what is the lateral performance of the specimens when lateral loading is applied to the specimens under investigation instead of axial loading? The problem is that the load path is applied to the specimens laterally instead of axially as a displacement control. For a better comparison of the specimens, specimens were selected where the number of stiffeners was constant, so all specimens with 8 stiffeners (specimens "T8-4", "T8", "Box8", "Cir8" and "Tra8") were selected for lateral loading. Figure 34 shows the von Mises stress of the specimens studied.

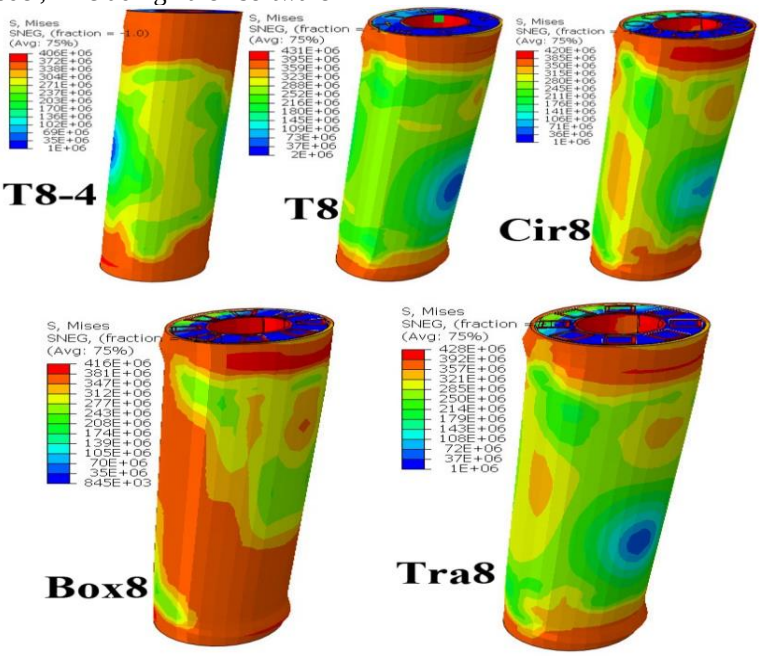

Figure 34 - Von Mises stress of lateral loading in the concrete filled double shell steel column specimens with 8 stiffeners (specimens "T8-4", "T8", "Box8", "Cir8" and "Tra8").

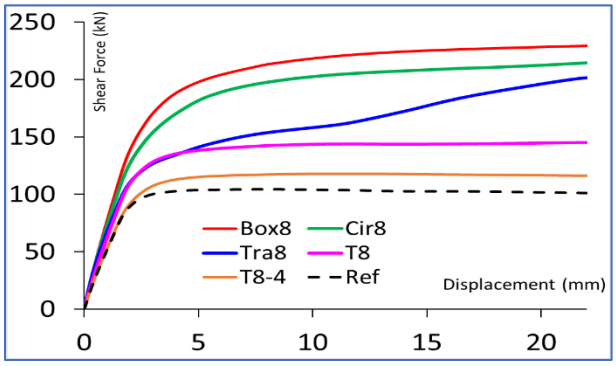

Figure 35 - Comparison of lateral load-displacement diagrams of concrete filled double shell steel columns with 8 stiffeners (samples "T8-4", "T8", "Box8", "Cir8" and "Tra8")

Meanwhile, Figure 34 shows the results of the lateral force-displacement diagram and the lateral performance information table for the specimens tested.

As can be seen in Figure 36, the lateral performance of the specimens studied, which include double-shell steel columns filled with concrete with 8 stiffeners "T8-4", "T8", "Box8", "Cir8" and "Tra8", are different from each other, which proves that the stiffener shape (assuming a constant number of stiffeners) is effective in their lateral performance. For a more detailed examination, Figure 37 shows the sorted relative lateral performance, which involves dividing the performance of each specimen by the performance of the base specimen, in three parts: relative lateral strength, relative lateral stiffness and relative lateral ductility.

The results of the relative lateral performance of the concrete-filled double-shell steel column specimens with 8 stiffeners (specimens "T8-4", "T8", "Box8", "Cir8" and "Tra8") compared to the base specimen show the effect of the stiffener shape (assuming a constant number of

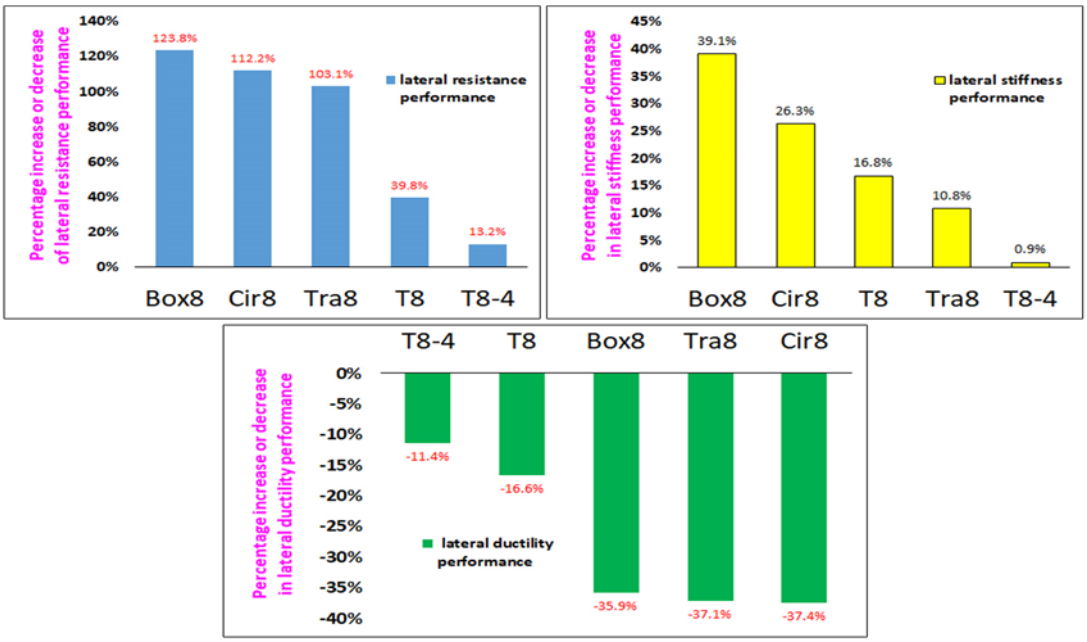

Figure 36 - Comparison of the lateral relative performance of concrete-filled steel tube columns with eight internal stiffeners (samples "T8-4," "T8," "Box8," "Cir8," and "Tra8") compared to the baseline sample.

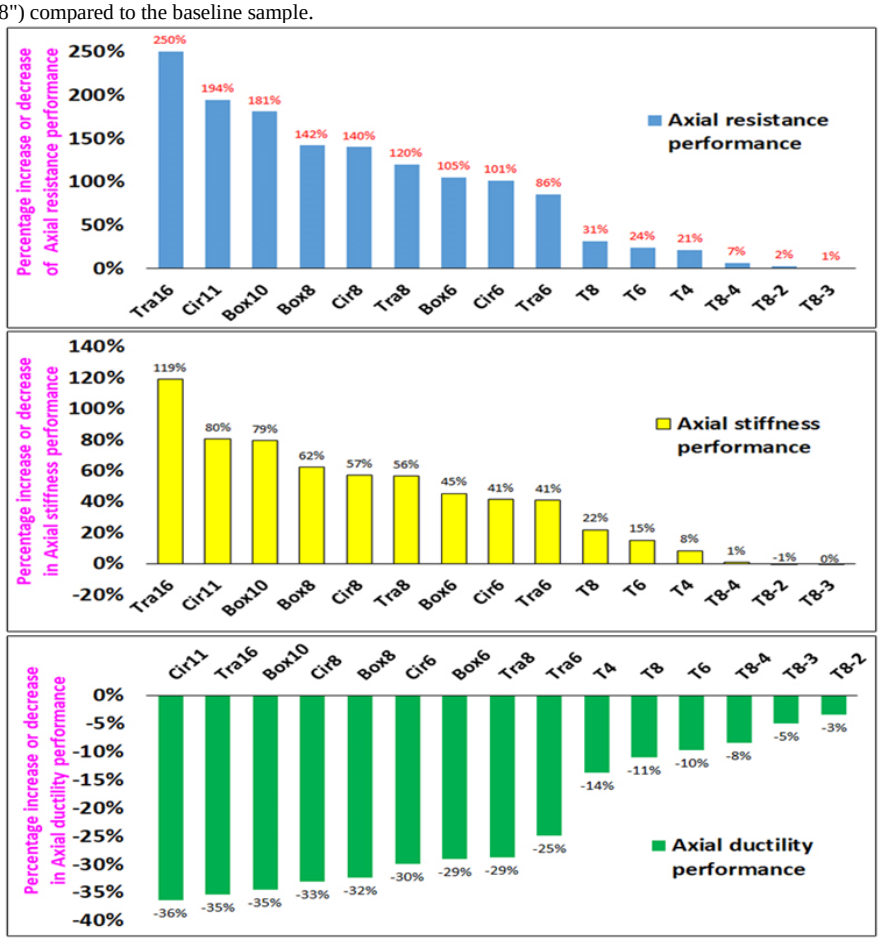

Figure 37 - Comparison of relative axial performance of all samples of double-shell steel columns filled with concrete with internal stiffener compared to the base sample

stiffeners), the details of which are presented in Chapter 5 of this study.

3.7. Investigation of the axial performance of the concrete-filled double-shell column and types of stiffeners

In this part of the study, which is also the final part of the research findings, the issue of comparing the axial performance of all the specimens under study is addressed. Therefore, the axial performance of all the specimens under study is shown along with the percentage increase or decrease in the axial performance compared to the base specimen (relative performance). The axial performance of the specimens under study, which includes concrete-filled double-shell steel columns with internal stiffeners, is shown. For a more detailed examination, in Figure 38, the sorted relative axial performance, which includes dividing the performance of each sample by the performance of the base sample, is shown in three parts: relative axial strength, relative axial stiffness, and relative axial ductility. Translate

The results of the relative axial performance of all samples of double-shell steel columns filled with concrete with internal stiffener compared to the base sample indicate the effect of the stiffener on the axial performance, the details of which are presented in Chapter 4 of this study.

4. Conclusion

According to the study, it has been determined that if the space between the two shells (inner and outer) of a double-shell steel column is filled with concrete, its axial and lateral performance is greatly improved. (So that in this study, the axial performance, which includes strength, stiffness and ductility, is improved by 55, 65 and 334% respectively, and its lateral performance is improved by 19, 39 and 14%).

1. A notable point in filling the space between the two shells with concrete is the axial ductility performance of the double-shell steel column, and the reason for this can be related to the fact that when a bare steel column (without concrete) is subjected to pure pressure, after the axial strength of the column reaches the yield point, it undergoes distortion and premature buckling, and this causes a decrease in uΔ and its axial ductility is greatly reduced. On the other hand, the problem of premature buckling does not occur in a double-shell steel column filled with concrete, and as a result, its axial ductility performance is higher than that of the steel column sample. The bare steel column becomes much higher.
2. In the studies conducted on the stresses created in the samples and components of the double-shell steel column filled with concrete with internal stiffeners, it can be seen that in terms of axial loading, the inner shell, the internal stiffener, the outer shell and the concrete between the two shells have the largest share in load transfer, and in terms of lateral loading, the inner shell, the outer shell and the concrete between the two shells have the largest share in load transfer. Therefore, considering the high share of the internal stiffener in load transfer, it is possible to understand the importance of this issue.
3. The results of the research showed that by increasing the number of stiffeners in the height of the double-shell steel column filled with concrete, the axial strength and stiffness of the column increase, but its ductility decreases.
4. The research showed that the use of overall stiffeners in the double-shell steel column filled with concrete is preferable to sectional stiffeners, and the reason for this can be attributed to the direct participation of stiffeners in axial and lateral load transfer.
5. Research has also proven that instead of using all the energy spent on welding stiffeners in the column body, only placing stiffeners inside the space between the two shells (provided they fit) and pouring concrete results in better results in terms of axial and lateral performance.
6. The results show that by using square stiffeners inside the space between the two shells, double-shell steel columns filled with concrete have the best performance in terms of axial and lateral performance in terms of two criteria of strength and stiffness, but due to their geometric shape, a large number of these stiffeners cannot be used inside the space between the two shells, because these stiffeners collide with each other and cannot be placed in large numbers.
7. The results also show that in terms of axial and lateral performance in terms of two criteria of strength and stiffness, after the overall square stiffeners, there are two circular and trapezoidal shapes, respectively, and then finally the T-shape.
8. Research has shown that as the number of global stiffeners inside the space between the two shells increases, the axial and lateral performance in the two criteria of strength and stiffness also increases. In addition, the trapezoidal shape is the best shape for placing the stiffener inside the space between the two shells, so that in this research, 16 trapezoidal stiffeners, 11 circular

stiffeners, and 10 square stiffeners were placed inside the space between the two shells.

9. Research shows that using stiffeners inside the space between the two shells in a double-shell steel column filled with concrete reduces the axial and lateral ductility criteria, and columns with circular stiffeners showed the greatest reduction in ductility compared to the others.

References

[1] Ezoji, Reyhaneh. "A Review on Behaviour and Strength of Concrete Filled Steel Tubular Columns." Journal of Civil Engineering Researchers, vol. 1, no. 7, 2017, pp. 12–16.

[2] Hadi Faghihmaleki and Gholamreza Abdollahzadeh. “Using Risk-Based Robustness Index for Seismic Improvement of Structures.” KSCE Journal of Civil Engineering 23.3 (2019): 1207–1218. DOI: https://doi.org/10.1007/s12205-019-0350-5 .

[3] Hadi Faghihmaleki and Mohammad Sayadi. “Evaluation of the Performance of Moment Resisting Steel Frames under Near Field and Far Field Earthquakes Based on Energy Conception.” Sigma Journal of Engineering and Natural Sciences 40.1 (2022): 1–8. DOI: https://doi.org/10.14744/sigma.2022.00001 .

[4] Mohammadreza Noori Shirazi. “Seismic Strength of RC Columns Using Enhanced Steel Jacket. FE Modeling.” Journal of Civil Engineering Researchers 4.1 (2022): 39–54. DOI: https://doi.org/10.52547/JCER.4.1.39 .

[5] Zhiwei Ding, Faxing Li, Gang Gong, and Yuzhong Yu. “Behavior of Tubular Stub Columns of Axially Loaded Steel-Reinforced Concrete-Filled Circular Steel.” Journal of Central South University 43 (2012): 3625–3630.

[6] Ahmed Elremaily and Atorod Azizinamini. “Behavior and Strength of Circular Concrete-Filled Tube Columns.” Journal of Constructional Steel Research 58.12 (2019): 1567–1591. DOI: https://doi.org/10.1016/S0143-974X(02)00005-6 .

[7] M. V. Chitawadagi, M. C. Narasimhan, and S. M. Kulkarni. “Axial Capacity of Rectangular Concrete-Filled Steel Tube Columns – DOE Approach.” Construction and Building Materials 24.4 (2010): 585–595. DOI: https://doi.org/10.1016/j.conbuildmat.2009.09.006 .

[8] Zhong Tao, Brian Uy, Feiyan Liao, and Lianghua Han. “Nonlinear Analysis of Concrete-Filled Square Stainless Steel Stub Columns under Axial Compression.” Journal of Constructional Steel Research 67.11 (2021): 1719–1732. DOI: https://doi.org/10.1016/j.jcsr.2011.04.012 .

[9] Mahmoud M. El-Heweity. “On the Performance of Circular Concrete-Filled High Strength Steel Columns under Axial Loading.” Alexandria Engineering Journal 51.2 (2022): 109–119. DOI: https://doi.org/10.1016/j.aej.2012.05.006 .

[10] Wenbin Yuan and Jinjun Yang. “Experimental and Numerical Studies of Short Concrete-Filled Double Skin Composite Tube Columns under Axially Compressive Loads.” Journal of Constructional Steel Research 80 (2023): 23–31. DOI: https://doi.org/10.1016/j.jcsr.2012.09.014 .

[11] Tamer Ekmekyapar, Omar H. Alwan, Hozan G. Hasan, Bashar A. Shehab, and Bashar J. M. AL-Eliwi. “Comparison of Classical, Double Skin and Double Section CFST Stub Columns: Experiments and Design Formulations.” Journal of Constructional Steel Research 155 (2019): 192–204. DOI: https://doi.org/10.1016/j.jcsr.2018.12.025 .